Struct Chem (2012) 23:1115–1120
DOI 10.1007/s11224-011-9864-2

ORIGINAL RESEARCH

Cluster packing from a higher dimensional perspective

Walter Steurer · Sofia Deloudi

Received: 29 June 2011 / Accepted: 9 August 2011 / Published online: 30 August 2011

Abstract The way to find the optimum packing of quasicrystal-constituting clusters is discussed based on the projected-cell approach. We illustrate why the quasiperiodic arrangement of partially overlapping clusters with decagonal or icosahedral symmetry is the most efficient one, by relating it to the packing of unit cells in hypercubic lattices.

Keywords Quasicrystal · Cluster · Packing · Higher-dimensional approach

Introduction

Quite a few stable decagonal and icosahedral quasicrystals (QC) have been identified so far in binary and ternary intermetallic systems (see, e.g., [1, 2] and references therein). Their structures, properties and stability have been intensively studied during more than a quarter century as testified by more than 10,000 publications to date. Nevertheless, it is still not fully understood why and how QC form, particularly in view of the fact that the same kind of clusters can constitute both QC and their periodic counterparts, the approximants. Furthermore, for many not directly involved in QC research, the powerful but arcane description of quasiperiodic structures as projections from hyperspace has still an aura of mystery. In the following, we will try to demystify the higher-dimensional approach by looking at the well-known strip-projection method from a different angle, demonstrating that its physical basis is in the cluster shape. This unusual view should also help sketching the big picture of QC formation.

We want to emphasize that the term "quasi" in connection with "crystal" has nothing to do with lack of order, it rather indicates the particular kind of order. The structural perfection of QC, as reflected in the width of X-ray diffraction peaks, for instance, is comparable to that of other complex intermetallic phases. This means that the global, overall structural correlation length can reach tens or hundreds of micrometers, despite the existence of some intrinsic local structural disorder. The idealized structure of QC is usually described in terms of a quasiperiodic tiling decorated by particular atomic arrangements or, equivalently, as quasiperiodic packings of multishell clusters. Here, the term "clusters" denotes fundamental structural units which may or may not be stabilized by chemical bonding [3, 4].

While the symmetry of the outer cluster shells usually reflects the overall symmetry of the QC, that of the inner shell(s) is frequently lower giving rise to structural disorder. We focus in this study only on the outer cluster shell(s), which determine the way of packing via shared structural subunits. We will explore how clusters with non-crystallographic symmetry can be packed in the topologically best possible way, i.e., without gaps and "glue atoms" filling them. One crucial boundary condition is that the local composition has to be as close as possible to the overall one.

It is well known that some regular and semiregular polyhedra, and even multi-shell clusters, can be described as projections of higher-dimensional polytopes (see e.g., [5, 6]). Consequently, it is obvious to treat the problem of the topologically best cluster packing from a higher dimensional perspective. For instance, every three-dimensional (3D) zonohedron with octahedral or icosahedral symmetry can be described as orthogonal projection of an nD

W. Steurer (✉) · S. Deloudi
Laboratory of Crystallography, Department of Materials, ETH Zurich, Wolfgang-Pauli-Strasse 10, 8093 Zurich, Switzerland
e-mail: steurer@mat.ethz.ch

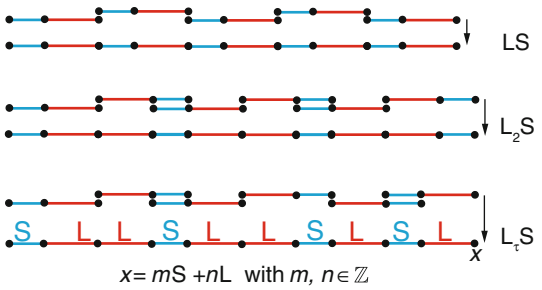

Fig. 1 Sequences with overall composition LS (*top*), L_2S (*middle*) and $L_\tau S$, i.e. the Fibonacci sequence (*bottom*), with the decomposition into covering clusters of the type (LS) in both orientations. The upper two sequences are rational approximants of the Fibonacci sequence

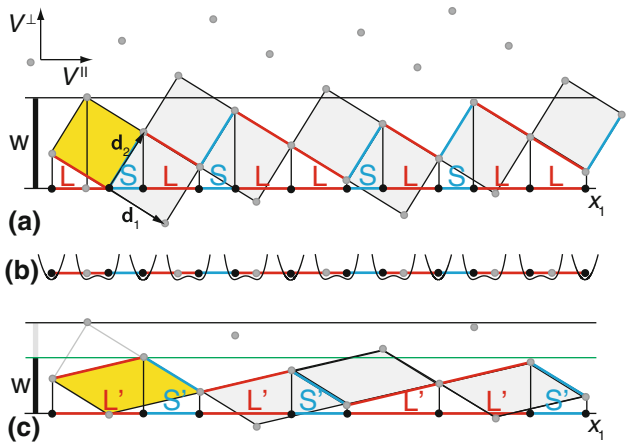

Fig. 2 Fibonacci sequence in the 2D description. (**a**) Projection of a sequence of vertex and edge connected shaded squares gives the FS plus some additional vertices (*grey*) at flip positions in a double-well potential (**b**). The size W of the strip defines the minimum distance between projected lattice points as well as the unit tile sequence; in our case, W is chosen so that the topmost vertex of the *yellow square* is outside the strip. Decreasing the acceptance window by a factor τ^{-1} leads to a scaling of the intervals L and S by a factor τ yielding the sequence L′S′L′S′L′L′S′, with $L' = L + S$ and $S' = L$ (**c**) (Color figure online)

hypercube [5]. Thereby, the number of edge directions of the respective zonohedron defines the dimension n; this gives, for instance, $n = 6$ for the triacontahedron. The assembly of such zonohedra with optimum density (frequency in a given volume) for a given chemical composition is a non-trivial problem that can be tackled much more easily in higher dimensions. Columnar clusters with, in projection, octagonal, decagonal or dodecagonal shape can be related to 2D projections of nD ($n = 4, 5, 6$) hypercubes.

In order to introduce our basic concept, we will start the discussion with a cluster leading to the simplest quasiperiodic structure, the 1D Fibonacci sequence (FS). Subsequently, we will move on to decagonal and triacontahedral clusters whose packing results in the 2D Penrose (PT) and 3D Ammann tiling (AT), respectively.

(LS) Cluster and Fibonacci sequence

Let us assume that we have an energetically favorable 1D cluster, (LS), consisting of atoms at the vertices of a vertex-sharing assembly of a long interval L and a short interval S, with length ratio $L = \tau S$ and $\tau = 2\cos(\pi/5)$. In a structure (sequence, tiling), this cluster can occur in both orientations, (LS) and (SL). While …LL… and …LS… neighbours in a structure should be energetically favorable, …SS… neighbors should be strongly discouraged. Depending on the overall stoichiometry, different structures result as illustrated with the three examples shown in Fig. 1.

On top of Fig. 1, a part of the infinite sequence …(LS)(LS)(LS)… = …LSLSLS… is depicted for an overall composition LS. The clusters, with the same stoichiometry as the whole sequence, are put together just by sharing vertices. All alternative structures with the same stoichiometry that contain …SS… neighbors are energetically less favorable. The most disadvantageous case would be the sequence …(LS)(SL)(LS)(SL)… = …LSSLLS SL… with 50% SS neighbors. In the middle of Fig. 1, a sequence is drawn with overall composition L_2S, which differs from the cluster stoichiometry LS. The only way to realize this composition is by allowing cluster overlaps of the type (L(S)L) yielding the sequence …(L(S)L)(L(S)L) … = …LSLLSL… Finally, at the bottom of Fig. 1, the sequence with overall composition $L_\tau S$ is shown. It is part of the Fibonacci sequence, a substitutional sequence resulting from iterative substitution operations acting on an alphabet (L, S): L ⇒ LS, S ⇒ L. For approaching locally the overall composition as close as possible, an (LS) cluster assembly with both vertex and S sharing is needed. However, it would be difficult, if not impossible, to piece together the FS based on this information alone without knowledge of the substitution rule. Fortunately, this problem can be easily solved in 2D space.

For this purpose, we describe the covering cluster (LS) as projection (shadow) of a properly oriented square (shaded in Fig. 2a). Of course, we could use any parallelogram provided it had the same shadow. The topmost and the lowermost vertices of the square project into the interval defined by the left and right vertex and create so-called flip positions. Accepting the interval S as the shortest possible interatomic distance, the two flip positions, with a distance S/τ cannot be occupied at the same time. This is illustrated in Fig. 2b by a double-well potential containing a black dot for an occupied flip position and a grey dot for an unoccupied one. If an atom is excited and jumps to the alternative position in the double well potential, then this corresponds to a so-called simpleton flip (LS) ⇔ (SL).

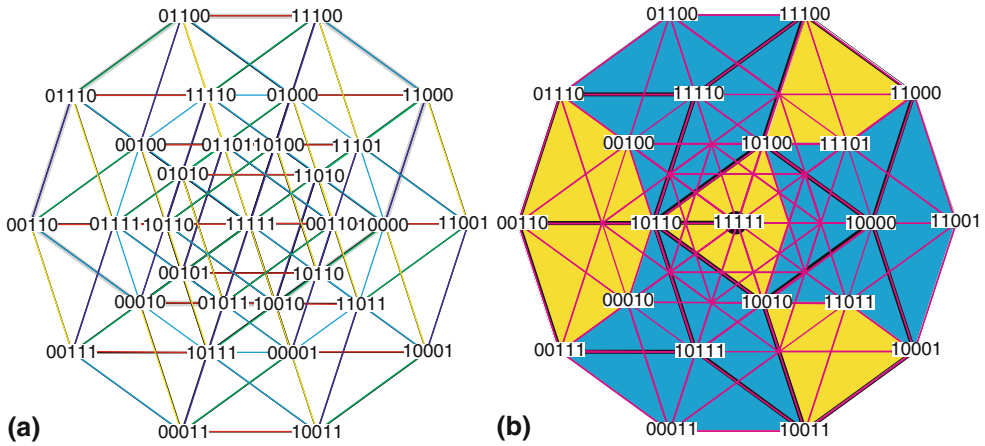

Fig. 3 5D hypercubic unit cell projected along its body diagonal [11111] onto 2D par-space. The vertices are indexed based on the 5-star of basis vectors, with each basis vector in a different color. The thick outlined polygon in (**a**) corresponds to the projection of the 4D face (subcube) with the last index equal to zero. Applying the minimum distance criterion by adjusting the acceptance window, we obtain a vertex distribution related to a decorated rhomb PT, for instance (**b**). The *blue-* and *yellow-colored* regions in (**b**) mark the overlap regions of the Gummelt decagon, a covering cluster of the PT (Color figure online)

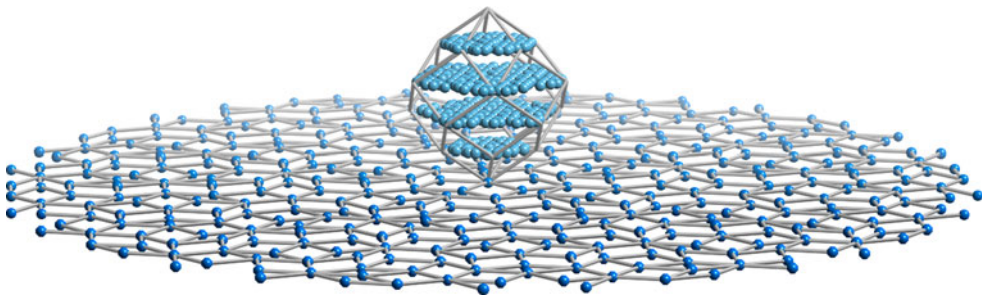

Fig. 4 Visualization of 5D space showing 2D par-space and 3D perp-space projections, i.e. a decorated PT (*dark blue spheres*) and its acceptance window (an *elongated rhombic icosahedron*), connected via the common origin. The nodes of the 5D hyperlattice, with par-space values in the range of the PT shown, form in their perp-space projection the four pentagons inside the acceptance window (*light-blue spheres*) (Color figure online)

As illustrated in Fig. 2a, two-cluster sequences of the type (SL)(LS) = SLLS can be obtained by projecting the vertices of compounds of two vertex-sharing squares. The cluster density amounts to $d_{\text{cluster}} = 2/2 = 1$. Overlaps of the type (L(S)L) = LSL result from two squares sharing an S-generating edge. The resulting local cluster density is higher in this case, $d_{\text{cluster}} = 2/3$. The cluster-generating squares can be seen as unit cells of a 2D lattice spanned by the basis vectors $\mathbf{d}_1 = a(cos\,\pi/5,\ -sin\,\pi/5)_{\text{V}}$ and $\mathbf{d}_2 = a(sin\,\pi/5,\ cos\,2\pi/5)_{\text{V}}$ (D-basis), defined on a Cartesian coordinate system (V-basis); $x_1^{\text{V}}$is the V-basis coordinate in physical or par(allel)-space $\text{V}^{\parallel}$, x_2^{V} refers to perp(endicular)-space $\text{V}^{\perp}$. One obtains the cluster components L = $\mathbf{Pd}_1$, S = $\mathbf{Pd}_2$ with the projection matrix.

$$\mathbf{P} = \begin{pmatrix} 1 & 0 \\ 0 & 0 \end{pmatrix}. \tag{1}$$

The projection of one unit cell onto the perp-space gives the acceptance window W and, therewith, the width of the strip defining the subset of lattice nodes of the tiling. Consequently, its size also determines the minimum distance between the projected lattice nodes. In order to eliminate flip positions, W has to be chosen so that either the topmost (as in our example) or the lowermost vertex of the yellow square comes to lie outside the strip. Then the FS can be obtained as projection of the vertices of an infinite vertex- and edge-connected, respectively, sequence of squares out of a 2D lattice lying within a strip of width W (Fig. 2a).

Generally, the vertices of quasiperiodic tilings correspond to a subset of a $\mathbb{Z}$-module (vector module with integer coefficients) of rank n, depending on the number n of basis vectors needed to index the vertices with integers. Any $\mathbb{Z}$-module can be seen as proper projection of an nD lattice onto the dD par-space. The minimum distance between the tiling vertices defines the width W of the strip that selects the lattice nodes to be projected. The acceptance window W is defined in the (n-d)D perp-space. A change in the strip width W always entails a change in the unit cell shape without changing the unit cell volume. This results in a scaling of the quasiperiodic structure as shown in Fig. 2c.

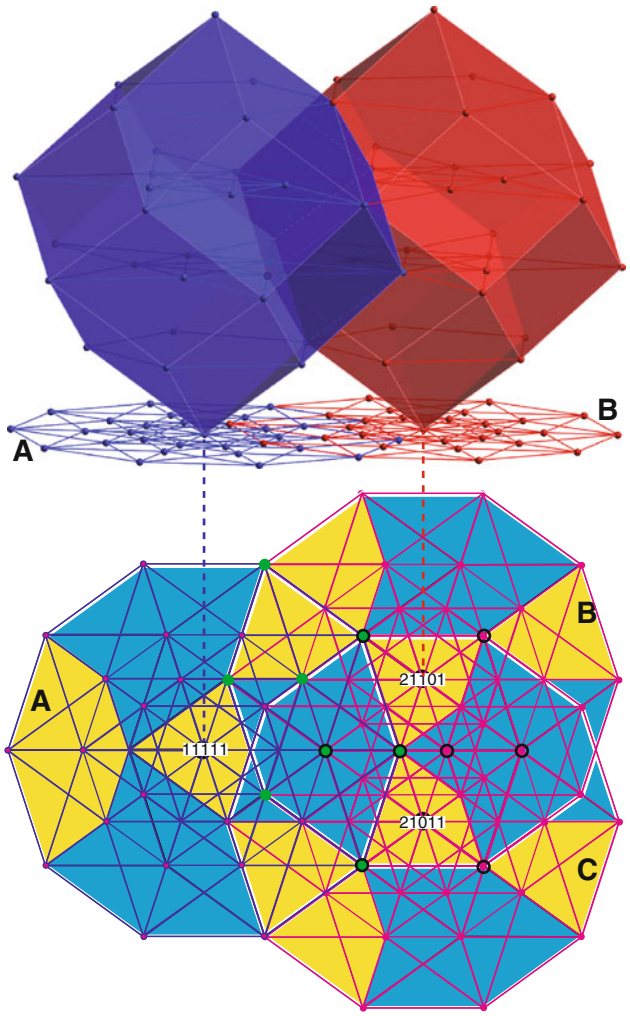

Fig. 5 *Top* 5D hypercubic unit cells, separated by the vector $(10\bar{1}00)_D$, in combined par-/perp-space projections giving elongated rhombic icosahedra and overlapping decagons A and B in the subspaces spanned by vectors $(10000)_V$, $(01000)_V$, and $(00001)_V$ and by vectors $(10000)_V$, $(01000)_V$, respectively. *Bottom* Three Gummelt decagons A, B, and C, with two different types of permitted overlaps. The centers of the decagons are separated by the vectors **a**–**b**: $(100\bar{1}0)_D$, **a**–**c**: $(10\bar{1}00)_D$ and the τ^{-1} times smaller one for **b**–**c**: $(00\bar{1}10)_D$. The corresponding 5D hypercubes share 3D faces containing 8 lattice points each. *Green dots* mark the shared vertices of the hypercubes related to the decagons **a** and **b**, *black circles* those of **b** and **c** (Color figure online)

A strip, meandering with a limited amplitude around the ideal par-space direction, not only leads to local changes in the structure (disorder) but also in the local L/S ratio. However, if the global stoichiometry is kept constant, the disordered structure will remain quasiperiodic on average.

Decagon cluster and 2D penrose tiling

Decagonal QC can be described as packing of partially overlapping decaprismatic columnar clusters. For the study of the different ways to pack these clusters in the quasi-periodic directions, it is sufficient to consider their 2D projections along the tenfold axis, i.e., the periodic direction. The resulting 2D cluster of decagonal shape can be described as projection of a 5D hypercube along one of its fivefold axes. 22 of its 32 vertices project into the interior of the resulting decagon (Fig. 3).

As before, we take this hypercube as unit cell of a 5D hyperlattice with basis vectors $\mathbf{d}_i = a(cos\,2\pi i/5,\ sin\,2\pi i/5,\ cos\,4\pi i/5,\ sin\,4\pi i/5,\ 1/\sqrt{2})_V, \quad 1 \le i \le 5$ (D-basis); x_i^V with $1 \le i \le 3$ are Cartesian coordinates in par-space, those with $i = 4, 5$ in perp-space. The projection of the 5D hypercubic unit cell onto 3D perp-space yields the acceptance window W for the generation of the 2D PT, an elongated rhombic icosahedron (Fig. 4). All hyperlattice points, which fall into this acceptance window if projected onto perp-space, are located inside the strip and generate the PT by par-space projection. The rhombic icosahedron is elongated along its fivefold axis compared to the zonohedron with the same name. Furthermore, its faces with a vertex on the fivefold axis are not congruent to the other ones.

In order to find the most efficient way of packing decagon clusters, we have to analyze the different connectivities of the unit cells in the strip cut out of the 5D hypercubic lattice by the acceptance window W. In 3D, neighboring unit cells can share 2D faces, 1D edges or 0D vertices. In a 5D hyperlattice, they can additionally share 4D or 3D faces with 16 or 8 joint vertices, respectively. The overlap rules of the 2D decagons result from the ways the projected hypercubic unit cells can overlap. In case of the Gummelt decagon [7], the assemblies with allowed overlaps, as defined by the the rocket decoration (blue areas in the overlapping decagons shown in Fig. 5), all result from the projection of 5D hypercubic unit cells sharing 3D faces (8 lattice nodes). A higher decagon cluster density would result from the projection of hypercubic unit cells sharing 4D faces (16 lattice nodes), which are shifted against each other by one lattice translation of the type $(10000)_D$. Such a shared area is shown in Fig. 3a. It is not allowed in the ideal PT, but it can be observed as defect in decagonal quasicrystals.

In Fig. 5 (top), a combination is shown of the par- and perp-space projections of two 3D-face-sharing 5D unit cells, separated by the vector $(10\bar{1}00)_D$: the elongated rhombic icosahedra result from the projection onto the subspace spanned by vectors $(10000)_V$, $(01000)_V$, and $(00001)_V$ and the decagons from the projection onto the $(11000)_V$ plane. The vertices that are projected onto equidistant hyperplanes inside the elongated rhombic icosahedra stem from 4D hyperlattice planes with indices $(m_1\ m_2\ m_3\ m_4\ m_5)_D$ with $m_5 = 0, 1, 2,\ldots$

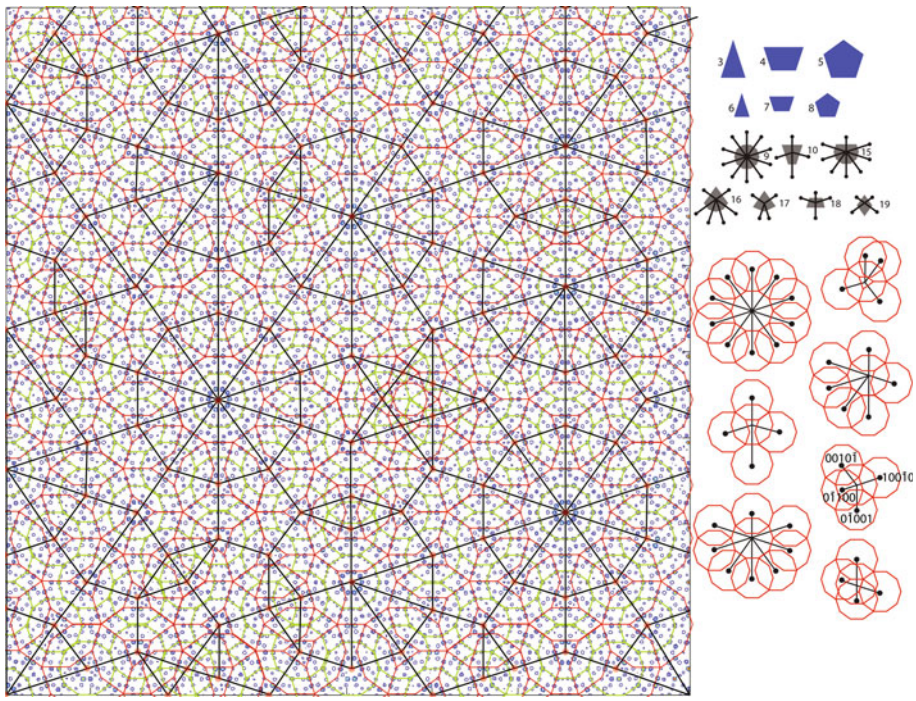

Fig. 6 Projected electron density distribution function of decagonal Al–Ni–Rh (courtesy of D. Logvinovich, LFK, ETHZ) with ≈20 and ≈12 Å decagon clusters marked red and green, respectively. The decagon centers are located on the vertices of a DT_5/VT_{13} Masakova tiling [8]. At *upper right*, the Delone and Voronoi tiles are shown (numbering according to [8]), *shaded blue and grey*, respectively, and below, the different vertex configurations and decagon cluster overlaps. For one vertex configuration the lattice translations are given between neighboring 5D unit cells corresponding to the respective overlapping decagons (Color figure online)

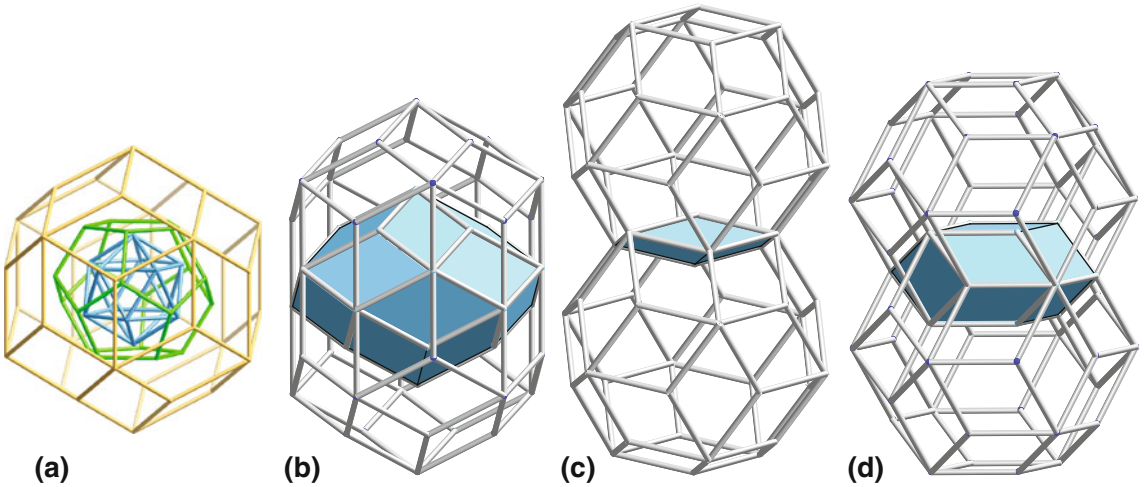

Fig. 7 **a** 6D hypercube projected onto 3D par-space. Its 64 vertices project onto the 32 vertices of a triacontahedron (*yellow*), to the 12 vertices of the second shell, a dodecahedron (*green*), and to the 20 vertices of the innermost shell, an icosahedron (*blue*). **b–d** Shared regions of triacontahedra overlapping along the fivefold, threefold and twofold axes, respectively, **b** rhombic icosahedron, **c** oblate rhombohedron, and **d** rhombic dodecahedron (Color figure online)

Let us have a look at an example of a real decagonal QC in the system Al–Ni–Rh and see how the cluster concept applies to it. As shown in Fig. 6, the projected electron density distribution function can be covered by copies of a decagonal cluster with ≈20 Å diameter (red). The centers of the decagons form the vertices of a DT_5/VT_{13} Masáková tiling [8], created from one decagonal acceptance window in the 5D description. The Rh atoms are located on τ^{-1}-times smaller decagons (green) centered at the same positions as the larger ones (red). The shapes of the overlap areas of the large (red) covering decagon clusters are the same as those of the Gummelt decagons, however, their locations on the decagons and combinations are different. The smaller (green) decagons overlap less frequently and only with hexagon overlap areas; mostly they just share edges. The different cases of overlapping decagons can be related to neighboring unit cells of the 5D hypercubic lattice. For one vertex configuration the respective lattice translations are listed in Fig. 6 (bottom right).

The packing of the decagonal clusters can be explained by competing interactions. On one hand, the large decagons have very large overlap regions, on the other hand small

decagons just share edges occupied with Rh atoms. The edges of the Voronoi cells can be seen as local reflection lines that relate overlapping decagons by mirror symmetry.

Triacontahedron cluster and 3D Penrose (Ammann) tiling

The triacontahedron, an Archimedean solid dual to the icosidodecahedron, can be described as projection of a 6D hypercube along its fivefold axes onto 3D space (Fig. 7a). It is bounded by 12 5D faces, i.e. 5D hypercubes, which give in 3D projection rombic icosahedra. The lower-dimensional hyperfaces project into the respective diminished zonohedra: the 60 4D faces into rhombic dodecahedra and the 160 3D cells into cubes.

The possible overlap regions of two triacontahedra in each case are shown in Fig. 7b–d. The overlap along the fivefold axis results in a shared rhombic icosahedron. It corresponds to the projection of a compound of two 6D hypercubes, separated by a vector of the type $(100000)_D$ and sharing a 5D face with 32 vertices. The overlaps along the three- and twofold directions lead to an oblate rhombohedron and a rhombic dodecahedron, respectively, as shared volumes. The vectors between the 6D hypercubes are of the type $\left(00110\overline{1}\right)_D$ and $\left(0010\overline{1}0\right)_D$, corresponding to shared 3D faces with 8 vertices and 4D faces with 16 vertices, respectively. Consequently, taking the 6D hypercubes as unit cells of a hypercubic lattice and a strip analogously as defined before, then we obtain the densest possible packing of triacontahedral clusters, such as the Bergmann clusters, for instance.

If we remove one zone from the triacontahedron, we obtain a rhombic icosahedron. In projection along the fivefold axis onto 2D, a decagon cluster results as discussed before (see top of Fig. 5). The 6D embedding of decagonal phases allows to reveal structural relationships between decagonal and icosahedral phases in a straightforward way [9].

Conclusions

It is remarkable that the structures of decagonal and icosahedral QC are all closely related to the 2D PT and 3D AT, respectively, although they differ considerably in their chemical composition. However, this is not so surprising if we consider the structural similarities of their fundamental building clusters and, in particular, the way they can pack and overlap for particular stoichiometries. Obviously, a necessary but not sufficient condition for the formation of decagonal and icosahedral QC is the existence of clusters that can be described as proper projections of *n*D hypercubes, unit cells of *n*D hyperlattices. The optimum arrangement of the respective clusters in physical space corresponds to *n*D strips containing vertices of interlinked *n*D unit cells of the hyperlattice. Since the projection of such a strip gives a quasiperiodic structure, the densest arrangement of these particular clusters results to be quasiperiodic. However, if optimum cluster packing means the best packing of complete clusters then the strip cannot be straight but has to follow the boundaries of the *n*D unit cells. Of course, the average slope of this zigzag course has to be the same as that of the straight strip. In this case, the true structure could only be derived from electron microscopic images, which reflect the local structure properly. Higher-dimensional structure analysis is already based on the assumption of a straight strip. Therefore, it can give averaged structure information only.

References

1. Steurer W, Deloudi S (2008) Acta Crystallogr A 64:1–11
2. Steurer W, Deloudi S (2009) Crystallography of quasicrystals. Concepts, methods and structures. Springer series in materials science, vol 126. Springer, Heidelberg
3. Steurer W (2006) Philos Mag 86:1105–1113
4. Henley CL, de Boissieu M, Steurer W (2006) Philos Mag 86:1131–1151
5. Coxeter HSM (1973) Regular polytopes. Dover Publications, Inc, New York
6. Berger RF, Lee S, Johnson J, Nebgen B, Sha F, Xu J (2008) Chem Eur J 14:3908–3930
7. Gummelt P (1996) Geom Dedic 62:1–17
8. Masakova Z, Patera J, Zich J (2005) J Phys A 38:1947–1960
9. Mandal RK, Lele S (1991) Philos Mag B 63:513–527